Q. J. R. Meteorol. Soc. (2005), **131**, pp. 281–303 doi: 10.1256/qj.04.05

A new coupled chemistry–climate model for the stratosphere: The importance of coupling for future O_3-climate predictions

By WENSHOU TIAN and MARTYN P. CHIPPERFIELD*
Institute for Atmospheric Science, University of Leeds, UK

(Received 13 January 2004; revised 29 April 2004)

SUMMARY

We have created a new interactive model for coupled chemistry–climate studies of the stratosphere. The model combines the detailed stratospheric chemistry modules developed and tested in the SLIMCAT/TOMCAT off-line chemical transport models (CTM) with a version of the Met Office Unified Model (UM). The resulting chemistry–climate model (CCM), called UMCHEM, has a detailed description of stratospheric gas-phase and heterogeneous chemistry. The chemical fields of O_3, N_2O, CH_4 and H_2O are used interactively in the radiative heating calculation.

We present results from a series of 10-year 'time-slice' experiments for 2000 and 2050 conditions. The UMCHEM model performs well in reproducing basic features of the stratosphere. The distribution of long-lived tracers and 'age of air' compare well with observations. For O_3, the model tends to underestimate the stratospheric column at high latitudes by ∼20 DU. This is due to an underestimate of poleward transport in the mid-low stratosphere. The UMCHEM reproduces well the seasonal cycle in monthly mean column O_3 at mid-high latitudes, though the variability is slightly smaller than observations and smaller than in the SLIMCAT CTM. Other comparisons with the CTM, which has an identical chemistry scheme, show differences resulting from the models' meteorologies. For example, while the CTM reproduces the observed NO_y versus N_2O correlation, the UMCHEM overestimates the slope by about a factor of 2.

Including full chemistry in the UM causes important differences in the model's meteorology. As the zonal mean ozone climatology used in the UM is larger than that calculated in UMCHEM, with a maximum difference of 4 ppmv in the upper stratosphere, the UMCHEM temperature is about 4 K lower in the Antarctic lower stratosphere and 1–6 K higher in the upper stratosphere. The age of air is less in the basic UM by about 1–3 months in the lower stratosphere but slightly greater in the upper stratosphere. Coupling of the more realistic stratospheric chemistry water vapour warms the model stratosphere by ∼1–2 K. This water vapour coupling also results in a decrease in ozone with a maximum difference of about 250 ppbv in the tropical and southern high-latitude upper stratosphere, while in the tropical lower stratosphere ozone concentrations are increased by up to 30 ppbv.

For 2050 conditions, the model produces a column O_3 5% higher than present-day values in the tropics, about 15% higher in the Arctic winter/spring and up to 90% higher in the much smaller Antarctic O_3 hole. This large O_3 increase more than offsets the effect of cooling in the Antarctic late spring induced by greenhouse gases.

KEYWORDS: Ozone recovery Unified Model

1. INTRODUCTION

Understanding the causes of the observed past depletions of stratospheric ozone has been a major focus of atmospheric research over the past decades. Although some specific quantitative discrepancies remain, models can now capture many of the observed features of this depletion and can identify the role of anthropogenic halogen species in causing this (e.g. World Meteorological Organization (WMO) 2003). Now that stratospheric chlorine levels are decreasing, we expect the ozone layer to 'recover'. However, the timing and extent of this recovery is uncertain and depends on the interaction of atmospheric chemistry, dynamics and radiation with other climate variables. Robust predictions of the future recovery of stratospheric ozone need detailed, coupled three-dimensional (3D) atmospheric radiative–dynamical–chemical models.

Predictions of stratospheric climate require a general circulation model (GCM) which calculates radiation and dynamics. These models themselves are computationally expensive. However, over the past decade or so, many groups have made progress in including treatments of stratospheric chemistry in GCMs to produce coupled

* Corresponding author: School of the Environment, University of Leeds, Leeds LS2 9JT, UK.
e-mail: martyn@env.leeds.ac.uk

chemistry–climate models (CCMs) (e.g. Hein *et al.* 2001; Austin 2002). Given the cost of GCMs, and the relative lack of computer power even a few years ago, the detail of the chemistry that has been included is often very limited and even the most sophisticated schemes have made some notable approximations.

Meanwhile, the interpretation of past ozone changes has been greatly aided by the development of off-line 3D chemical transport models (CTMs). These models use winds and temperatures specified from meteorological analyses and so are not only constrained to 'real' meteorological situations but are computationally cheaper, allowing the inclusion of more detailed chemistry. Because of this, and their direct use in comparing with a wide range of observations, chemical schemes in CTMs are generally more detailed and somewhat more tested than those that have evolved in CCMs.

A summary of a range of recent experiments with state-of-the-art CCMs can be found in Austin *et al.* (2003) and WMO (2003). In these studies, CCMs were used to predict the future evolution of polar ozone and there were large differences between the models. Much of the differences are due to different predictions of the climate, but the models also contained widely differing treatments of chemistry. In fact, even CCMs which have otherwise detailed schemes can ignore, for example, bromine chemistry (e.g. Nagashima *et al.* 2002; Steil *et al.* 2003); such omissions make studies of polar O_3 loss semi-quantitative at best.

In this paper we describe the development of a new coupled CCM. This model is derived from the UK Met Office (UKMO) Unified Model (UM) GCM and the full 'stratospheric' chemistry scheme from the SLIMCAT/TOMCAT CTM (Chipperfield 1999). Our approach here has been to take complete code from the CTM, developed and tested over many years in CTM comparisons, and insert it in the UK Universities' community version of the UM GCM. By doing this, we plan to create a CCM with a chemical scheme detailed enough to represent all important interactions in the stratosphere and aid validation/testing of our new CCM by being able to compare the CCM with CTM runs.

The UM has already been used in studies with a stratospheric chemistry scheme over many years by Austin and co-workers (e.g. Austin *et al.* 1992, 2001; Austin 2002). However, here we have used our SLIMCAT/TOMCAT scheme as it is more comprehensive (e.g. more species and separate advection of all long-lived species) and builds on our past CTM work. The UM has also been used for coupled chemistry–climate studies with simple parametrized schemes for ozone (Braesicke and Pyle 2003) and CH_4/H_2O (MacKenzie and Harwood 2004).

Section 2 describes the Unified Model, gives details of our stratospheric chemistry scheme and summarizes the 10-year time-slice experiments performed for this paper. Section 3 then investigates the performance of the basic coupled model by comparing with observations and related SLIMCAT CTM output. Section 4 discusses the impact of the interactive coupling of chemical species, and in particular H_2O, on the model's radiation scheme. Section 5 describes coupled simulations for 2050 conditions. Our conclusions are presented in section 6.

2. Model and experiments

(*a*) *Met Office Unified Model*

The Met Office UM (Cullen 1993) is a hydrostatic, primitive-equation, grid-point atmospheric general-circulation model with a hybrid vertical coordinate. There are different versions of the model and in this study we have used the 'climate' version v4.5 L64. This model has a horizontal resolution of 2.5° latitude × 3.75°

TABLE 1. CHEMICAL SPECIES IN THE UMCHEM CHEMISTRY–CLIMATE MODEL

Category	Species
Coupled short-lived species	O_x {$=O_3 + O(^3P) + O(^1D)$} NO_x {$=N + NO + NO_2$}, NO_3, N_2O_5, HNO_3, HO_2NO_2, ClO_x {$=Cl + ClO + 2Cl_2O_2$}, $ClONO_2$, HCl, HOCl, OClO, BrO_x {$=Br + BrO$}, $BrONO_2$, BrCl, HBr, HOBr H_2O_2, CH_2O, CH_3OOH
Steady state	H, OH, HO_2, CH_3, CH_3O_2, CH_3O, HCO
Source gases	CH_4, N_2O, CO, H_2O, $CFCl_3$, CF_2Cl_2, CH_3Br
Aerosol	H_2SO_4
Fixed	O_2, N_2, H_2, CO_2

longitude and 64 vertical levels from the surface to 0.01 hPa (approximately 80 km). The vertical resolution in the stratosphere is ∼1.3 km.

This version of the UM uses the orographic gravity-wave drag scheme (Gregory *et al.* 1998) from the surface to 20 hPa. The scheme accounts for the anisotropy of subgrid orography in the calculation of the surface stress. Above 20 hPa, non-orographic gravity-wave drag is represented by a Rayleigh friction term. For the runs performed here, the model uses observed sea-surface temperatures (SSTs) from 2000 to 2002 to represent present-day conditions.

The UM uses the radiation scheme of Edwards and Slingo (1996) with some modifications in the middle atmosphere (Zhong and Haigh 2001). This scheme treats absorption by the gases CO_2, H_2O, O_3, N_2O, CH_4, CFC11 ($CFCl_3$), and CFC12 (CF_2Cl_2). In the standard UM, these gases are specified by climatological values.

In our version of the UM, the model's default tracer advection scheme has been replaced by the QUINTIC-MONO scheme (Gregory and West 2002). This scheme performs much better in maintaining realistic tracer distributions in the presence of strong gradients.

(*b*) *Chemistry scheme*

To create our coupled chemistry–climate version of the UM, we have taken the full stratospheric chemistry modules from the SLIMCAT/TOMCAT off-line 3D CTMs (Chipperfield 1999). This scheme has been developed for many years to be both comprehensive and computationally efficient. As well as being used in 3D CTM studies it has also been used in a 2D latitude–height model for 100-year simulations (e.g. Chipperfield and Feng 2003)—a useful test of the scheme's long-term stability.

The species contained in the model are listed in Table 1. The scheme contains all of the O_x, NO_y, Cl_y, Br_y and HO_x species believed to be important to describe stratospheric chemistry. The scheme also includes a detailed CH_4 oxidation scheme and a range of long-lived source gases. During the model simulations, the abundance of the three halogen-containing source gases ($CFCl_3$, CF_2Cl_2 and CH_3Br) are scaled to give the required chlorine/bromine loading (to account for the contributions from source gases not considered). The scheme uses 28 advected tracers in the UM (including a 'passive' O_x tracer to diagnose polar ozone loss). A list of chemical reactions in the scheme is given in Chipperfield (1999).

The model uses a limited number of chemical families for species which are in rapid photochemical equilibrium, and for which the partitioning can be calculated even at night (e.g. N, NO, NO_2). Otherwise, the species are integrated separately. For example, although OClO is photolysed rapidly during the day, it is not included in the ClO_x family as its concentration could not then be determined straightforwardly at night. To prevent a significant increase in computational cost on adding the source gases, these long-lived

species are integrated using a simple forward Euler integration scheme which is far cheaper than the semi-implicit scheme (Ramaroson *et al.* 1992) used for the shorter-lived species and families. Photochemical data are taken from Sander *et al.* (2000). To reduce computational costs, within the coupled CCM the chemistry is only calculated within a limited vertical domain (30 levels spanning 150 hPa to 0.5 hPa). Above and below this domain the chemical species are advected as passive tracers.

The photolysis rates (J values) are calculated using a scheme based on Lary and Pyle (1991), which in turn was based on Meier *et al.* (1982) and Nicolet *et al.* (1982). The scheme uses a 4D look-up table (which has coordinates of pressure altitude, temperature, O_3 column, and zenith angle) to interpolate precomputed J values to a particular location and time in the atmosphere. The scheme takes account of multiple scattering and spherical geometry and can calculate photolysis rates for zenith angles up to 96°, which is important for applications to the polar lower stratosphere.

For heterogeneous chemistry, the model contains an equilibrium treatment of reactions on liquid sulphuric acid aerosols and on solid nitric acid trihydrate (NAT) and ice particles. The treatment of liquid aerosols requires the H_2SO_4 loading of atmosphere. This field is updated by observed monthly values and advected as a passive tracer. For the time-slice experiments discussed here, a fixed month of January 1995 is used. The composition of liquid $H_2O/H_2SO_4/HNO_3/HCl$ aerosols is then calculated from the analytical scheme of Carslaw *et al.* (1995a,b) using this H_2SO_4 field along with the model fields of temperature and other chemical species. This scheme also calculates the solubilities of HBr, HOBr, and HOCl. The model calculates the equilibrium vapour pressure of H_2SO_4 following an expression of Ayers *et al.* (1980). This is then tested against the model H_2SO_4 field and used to switch off the liquid aerosol reactions in the upper stratosphere.

For NAT polar stratospheric clouds (PSCs) ($HNO_3.3H_2O$), the model mixing ratios of HNO_3, H_2O, and temperature are used with the expression of Hanson and Mauersberger (1988) to predict when they are thermodynamically possible. The available surface area is calculated from the amount of HNO_3 condensed assuming that there are 10 NAT particles cm^{-3}. Because NAT particles can be very large, gas diffusion limitation is taken into account (Turco *et al.* 1989).

Ice particles are assumed to form when they are thermodynamically possible. HNO_3 is removed from the gas phase in the presence of ice particles using the equilibrium NAT expression (Hanson and Mauersberger 1988). This assumes a NAT coating (as opposed to a liquid coating) to the ice particles. The available surface area is calculated from an estimate of the amount of H_2O which is condensed and assuming that the radius of the ice particles formed is 10 μm. In the current version of this model, there is no treatment of particle sedimentation and hence the model does not simulate polar denitrification or dehydration. In principle, the lack of denitrification in the coupled model will underestimate the PSC-related polar ozone loss and result in a slight overestimation of column ozone in the polar regions.

(*c*) *Coupled model experiments*

We have performed three 10-year 'time-slice' integrations with the coupled model (UMCHEM). These integrations use constant forcing for trace-gas mixing ratios at the lower boundary. The model runs are summarized in Table 2 and the trace-gas boundary conditions are given in Table 3. For run **R4**, which used 2050 boundary conditions, the greenhouse gas (GHG) values are from Intergovernmental Panel on Climate Change (2001) scenario A1B. The estimated halogen loadings are from WMO (2003). The meteorological initial conditions for 2050 were generated by running the

TABLE 2. SUMMARY OF 10-YEAR MODEL EXPERIMENTS

Run	Description	Source gases	Radiation coupling
UMC	Basic UM		None
R0	UMCHEM control	2000	O_3, N_2O, CH_4
R2	With stratospheric H_2O coupling	2000	O_3, N_2O, CH_4, H_2O
R4	Future conditions	2050	O_3, N_2O, CH_4

TABLE 3. CONCENTRATIONS OF GREENHOUSE GASES USED IN THE MODEL SIMULATIONS

Year	CO_2 (ppmv)	N_2O (ppbv)	CH_4 (ppbv)	CFC11 (pptv)	CFC12 (pptv)
2000	368	308	1760	262	540
2050	532	350	2400	105	350

UM for three years without chemistry, but with 2050 values of GHGs in the radiation scheme. It should be pointed out that both 2000 and 2050 runs used the same SST to suppress possible tropospheric responses. These full chemistry runs were initialized with output from a SLIMCAT CTM simulation for the appropriate 2000 or 2050 conditions. In addition to these three coupled runs, we have also performed a reference simulation of the basic UM without chemistry (run **UMC**).

We have used these four integrations to test the performance of the coupled model under present-day conditions (run **R0**), to investigate the effect of coupling interactive chemical species with the radiation scheme (runs **R0**, **R2** and **UMC**), and to investigate the main interactions between chemistry and climate in the 2050 atmosphere (runs **R0** and **R4**). All model diagnostics are 10-year averaged climatologies unless otherwise stated.

3. VALIDATION OF THE UMCHEM CLIMATOLOGY

In this section we compare the performance of the UMCHEM control run **R0** with observations and other suitable datasets. The Stratospheric Processes and their Role in Climate (SPARC) project has provided some reference global datasets (Randel *et al.* 2003), based on Upper Atmosphere Research Satellite (UARS) measurements which are well suited to test our coupled model. We also compare the UMCHEM output with the corresponding climatology from UKMO analyses (Swinbank and O'Neill 1994) and the SLIMCAT CTM output. Here we use results from a multiannual integration of SLIMCAT from 1989–2001 forced by European Centre for Medium-Range Weather Forecasts (ECMWF) ERA-40 and operational analyses which had a horizontal resolution of $7.5° \times 7.5°$. The inclusion of a SLIMCAT experiment enables us to diagnose insufficiencies in the UMCHEM chemistry and transport processes since it and SLIMCAT have the same chemistry module but different dynamics.

(*a*) *UM climatology*

Although our aim here is not to test the basic meteorology of the UM which is widely documented in other studies (e.g. Swinbank *et al.* 1998; Jackson *et al.* 2001), we do show a brief comparison of basic fields from our simulations. Figure 1 shows the UMCHEM climatology of temperature and zonal wind in comparison with the corresponding climatology from UKMO analyses. In June, temperatures in the Antarctic lower stratosphere in UMCHEM are about 5 K lower than the UKMO analyses;

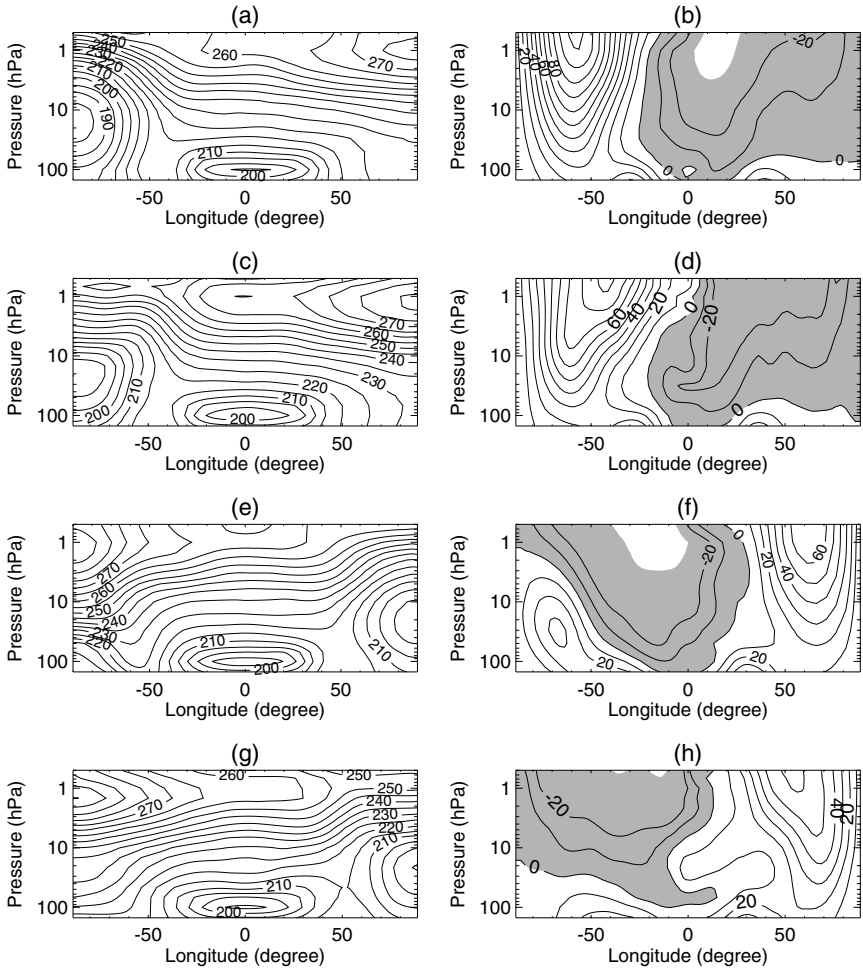

Figure 1. 10-year climatology of (a) zonal mean temperature (K) and (b) zonal mean wind speed (m s^{-1}, with negative (easterly) winds shaded) in June from the UMCHEM run **R0**; (c) and (d) are corresponding fields from UKMO analyses. (e) to (h) are as (a) to (d), but for December.

in the Arctic upper stratosphere, UMCHEM temperatures are about 5–10 K lower than UKMO. In the southern high-latitude upper stratosphere, the zonal wind from the UMCHEM is around 20 m s^{-1} larger than the UKMO analyses.

In December, UMCHEM temperatures in the Antarctic lower stratosphere are still ~5 K lower than UKMO while the temperature in the northern hemisphere (NH) upper stratosphere is higher than UKMO. In response to these temperature differences, the zonal wind in the southern high-latitude lower stratosphere in the UMCHEM is about 20 m s^{-1} larger than UKMO analyses.

The annual mean model temperature in lower-stratosphere southern high latitudes is about 5 K lower than the UKMO, while in the upper stratosphere the model temperature is overall higher than UKMO climatology (not shown). Clearly, the so-called 'cold pole bias' also exists in our coupled model, particularly in the Antarctic winter. This cold pole bias gives rise, via the thermal wind relation, to a polar jet in the model which is about 20 m s^{-1} stronger than that of UKMO climatology. More detailed evidence

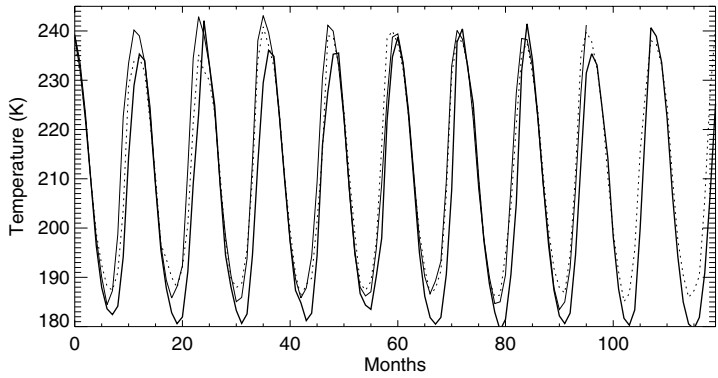

Figure 2. Time series of stratospheric monthly mean temperature (averaged between 100 and 10 hPa) at 85°S from ECMWF analyses (January 1984 to December 1993, dotted), UMCHEM output (January 1992 to December 1999, bold solid), and UKMO data (November 1991 to February 2000, thin solid).

about the model temperature bias in the Antarctic can be seen from Fig. 2, which shows the time series of the Antarctic polar stratospheric monthly mean temperature derived from three different datasets. Throughout the time period examined, the model minimum temperatures are about 2–5 K lower than those of UKMO and ECMWF. The model maximum temperatures are more in accordance with those of the UKMO and ECMWF, but overall are still lower.

Note that the 'cold pole problem' is a common feature in many climate models with a fully resolved stratosphere. It has been reported that using non-orographic gravity-wave drag (GWD) schemes in climate models can result in a significant reduction in the cold pole problem relative to Rayleigh friction (RF) schemes which act to decelerate the polar night jet (e.g. Manzini and McFarlane 1998). Manney *et al.* (2002) also found in their mechanistic model simulations that using RF to parametrize GWD in their model results in an unreasonable latitudinal structure of the upper-stratospheric jet. However, their results also suggest that a GWD scheme is likely to affect planetary-wave properties in the middle stratosphere, such as phase and amplitude. Meanwhile, due to interannual and interhemispheric variability in gravity-wave activity, inclusion of GWD in a model needs expensive tuning (which often has no physical foundation) to find an optimal set of GWD parameters. Although a good description of the gravity wave–stratospheric vortex interaction has important implications for predictions of ozone depletion and climate change, the topic is still under considerable debate (e.g. Duck *et al.* 2001). In our UMCHEM simulations, we have employed traditional RF as a gravity-wave proxy rather than a sophisticated GWD scheme. As discussed in section 4, inaccurate prescriptions of the Antarctic ozone climatology in GCMs without coupled chemistry may also affect those cold biases.

(*b*) *Tracer transport and age of air*

The age of air is a very useful diagnostic of tracer transport although direct inference of the mean age of air from observations is not straightforward. In CCMs and CTMs, the mean age of air can be calculated from the age spectrum by using an age tracer in the model. In theory, the stratospheric response to a pulsed mixing-ratio boundary condition at the model surface gives the age spectrum (Waugh and Hall 2002). The configuration for the age tracer in our experiments is the same as that described in Hall *et al.* (1999), namely within the latitude band ±10° and surface to 850 hPa, the mixing ratio of a

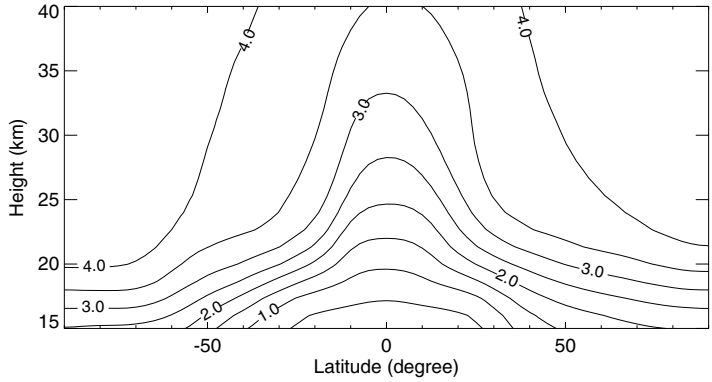

Figure 3. Zonal mean cross-section of mean age (years) from the UMCHEM run **R0**.

passive tracer was set equal to 1 during the first January and then equal to 0 for rest of the 10-year run.

Figure 3 shows that the mean age of air from the UMCHEM, e.g. maximum age in the high-latitude upper stratosphere of 4–5 years, is well within the range of the mean ages derived from the observations and model simulations shown by previous authors (see Hall *et al.* 1999), suggesting that the long-term tracer transport in the coupled model is overall reasonable. The mean age in Fig. 3 is similar to, but slightly less than, that derived by Mackenzie and Harwood (2004) using their version of the UM. These age differences may be caused partly by the new tracer advection scheme we used in the model. However, it is also possible that different radiation coupling can cause a response in the transport process. The effect of different radiation coupling on the modelled age of air is discussed in section 4(a).

Further information about the transport process in the UMCHEM can be gained from the model tracer fields. Latitude–height cross-sections of the 10-year averaged zonal mean O_3 and CH_4 fields from the UMCHEM and SLIMCAT are shown in Fig. 4 in comparison with the corresponding SPARC climatology. For CH_4 the basic features of the UMCHEM distribution are consistent with UARS observations. The UMCHEM has a good representation of the tropical ascent and strong tracer gradients in the subtropics. The CH_4 mixing-ratio contours are broadly in accordance with those of the age of air (Fig. 3). In the high-latitude upper stratosphere, the UMCHEM strongly overestimates the observed low mixing ratios of less than 0.2 ppmv. In contrast, the SLIMCAT CTM captures these values because in the CTM run the chemistry extended to 0.1 hPa. For the UMCHEM runs there is no chemistry above 0.5 hPa (i.e. CH_4 is a passive tracer above this altitude) and so the model has too much CH_4 in air descending from the mesosphere.

Both the UMCHEM and SLIMCAT show a good capability in reproducing the stratospheric ozone field, although the mid-stratosphere ozone maximum in SLIMCAT, which will have the more realistic temperatures, is slightly underestimated compared with the UARS observations. In the middle stratosphere the UMCHEM contours do not extend as far poleward as those of the SPARC data or SLIMCAT.

(*c*) *Column ozone*

To verify the reliability and stability of the coupled model, the time series of total-column ozone from the control integration **R0** is shown in Fig. 5 along with Total Ozone Mapping Spectrometer (TOMS) observations. It should be noted that the UMCHEM

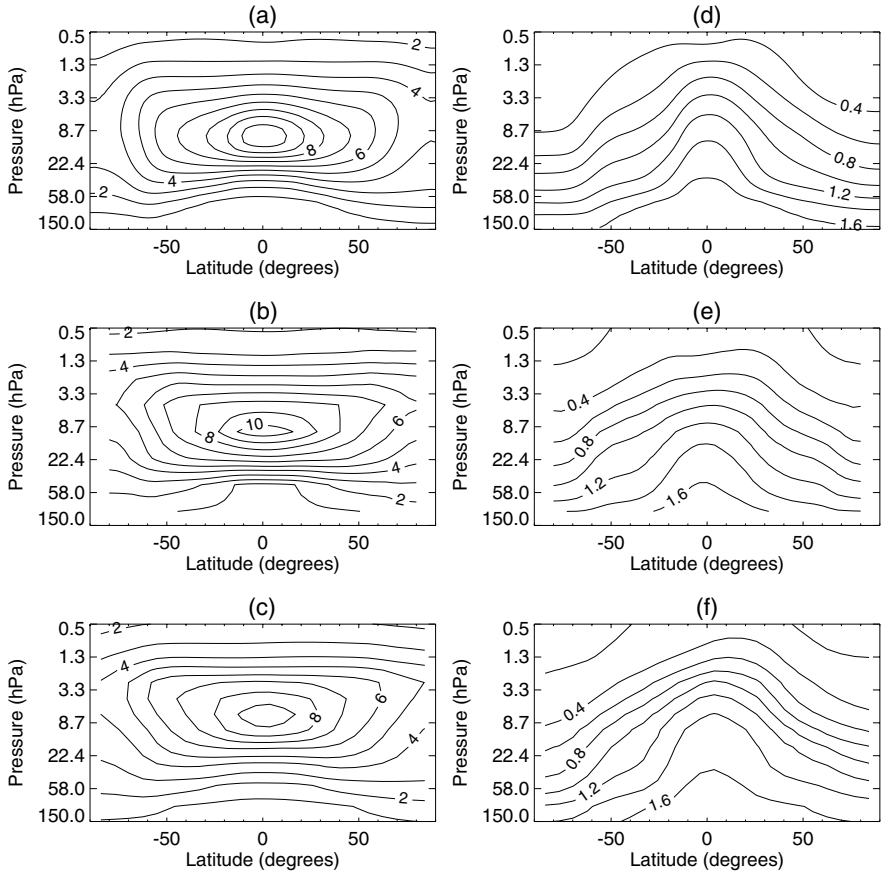

Figure 4. Latitude–height cross-sections of zonal mean O_3 (ppmv) from (a) the UMCHEM run **R0**, (b) the SPARC UARS climatology and (c) SLIMCAT. (d) to (f) are as (a) to (c), but for CH_4 (ppmv).

column ozone output only includes the 30 chemistry levels from 150 to 0.5 hPa and so the column contribution below this has been added based on the ozone climatology from Logan (1999). It is apparent that general characteristics of column ozone are well captured by the model with maxima in the NH spring mid-high latitudes and minima in the northern summer high latitudes. In the southern hemisphere (SH) the Antarctic ozone hole is evident with a clear annual cycle which is essentially the same as the TOMS data. The UMCHEM shows a slight underestimation (∼20 DU) of the total-column ozone in the northern high latitudes and an overestimation in midlatitudes and in the tropics. Further comparisons with 10 years of SLIMCAT output (from 1991 to 2001) reveal that there is no significant underestimation of column ozone by SLIMCAT in the northern high latitudes. This suggests that the underestimation of total-column ozone at the northern high latitudes is largely related to dynamics rather than chemistry since the UMCHEM and SLIMCAT show no similar underestimation of total-column ozone values at the same latitudes. The underestimation in the high-latitude column ozone is consistent with the lack of poleward extension of the O_3 contours in Fig. 4.

Figures 6(a) to (d) show the seasonal variation of total-column ozone at four different latitudes (again the tropospheric contribution of column ozone was added to the corresponding UMCHEM values). The UMCHEM captures the seasonal variation well

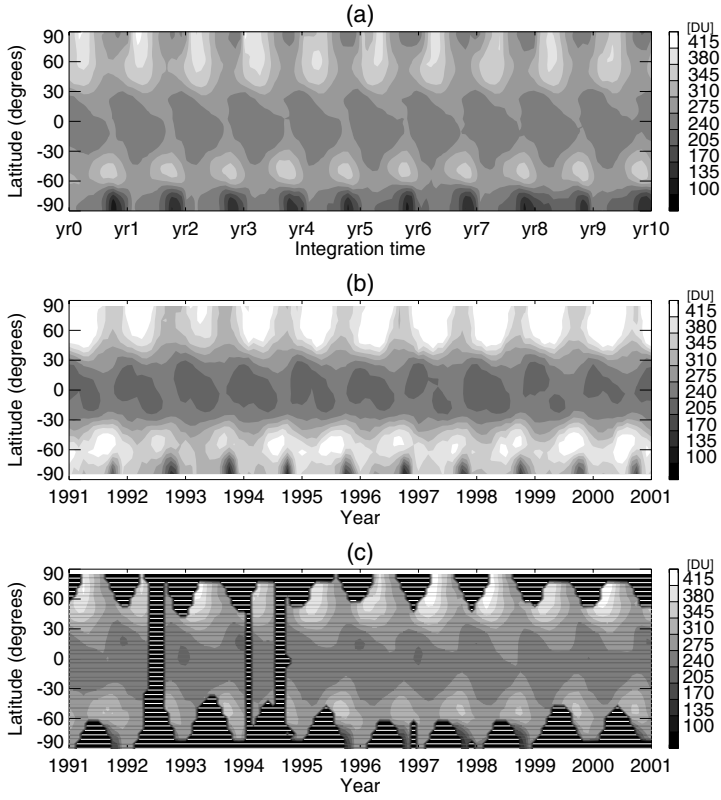

Figure 5. Time series over 10 years of zonal mean total-column ozone from (a) the UMCHEM run **R0**, (b) SLIMCAT and (c) TOMS observations. The TOMS data have periods of missing data between 1992 and 1995.

at these latitudes and, when the tropospheric contribution is included, compares well in magnitude with TOMS. For SLIMCAT the modelled O_3 column, especially in high latitude winter/spring depends on the analyses used to force the model and this early run with ERA-40 winds shows larger values than TOMS, e.g. a mean of 500 DU in spring at 65°N. The column ozone from SLIMCAT, which is driven by analysed winds, exhibits the largest interannual variability while the UMCHEM gives the smallest variability. Overall, these comparisons of two models with the same chemistry scheme emphasize the importance of dynamics in reproducing column ozone.

Some more information on the model's dynamical performance can be gained from comparing the seasonal variation of the stratospheric temperature with UKMO and ECMWF analysis (Figs. 6(e) to (h)). The model temperature in midlatitudes is about 0–5 K higher than those of UKMO and ECMWF. However, at the higher latitudes, the model mean temperature is in good agreement with UKMO and ECMWF analyses. There are no significant differences in temperature variabilities between the three datasets.

(*d*) *Tracer–tracer correlations and mixing*

In the stratosphere long-lived tracers, even when they are not chemically related, will exhibit compact correlation curves (Plumb and Ko 1992). These plots are a useful way of comparing observations and models, especially when the datasets are large or do not correspond to the same time period.

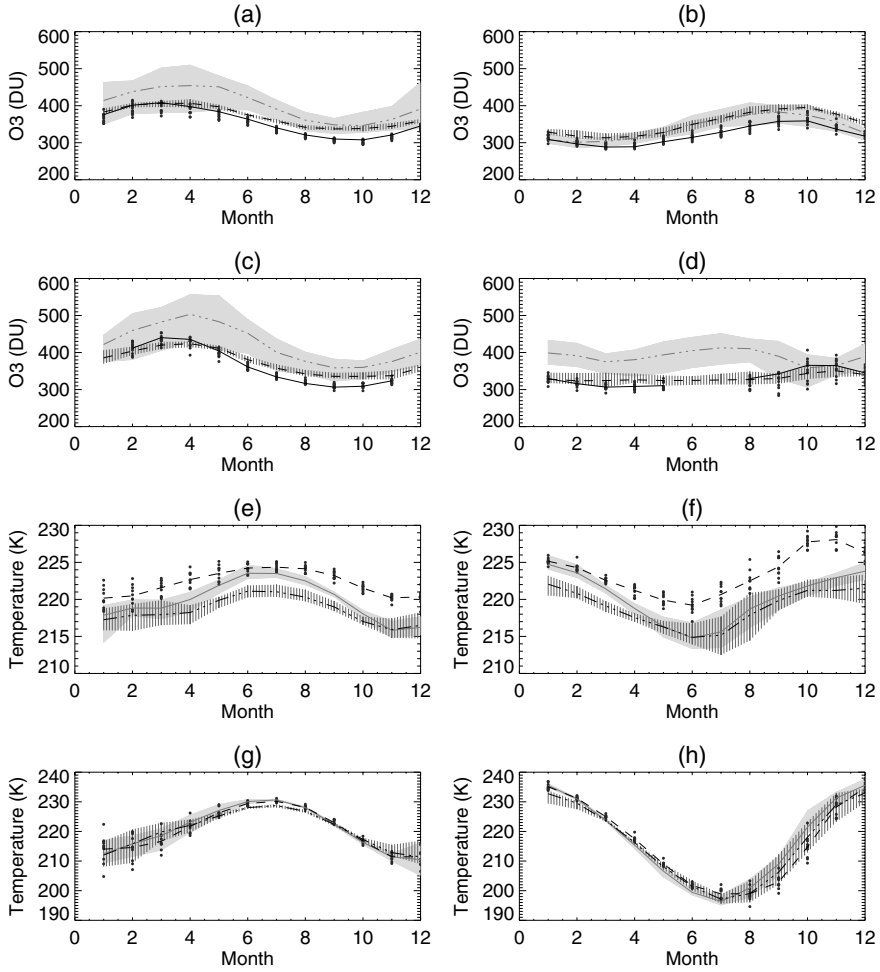

Figure 6. The seasonal variation of mean and variability (range) of total-column ozone at latitudes (a) 45°N, (b) 45°S, (c) 65°N and (d) 65°S for the UMCHEM (mean dashed line and variability vertical shading), TOMS data (mean solid line and variability dots), and SLIMCAT (mean dash-dotted line and variability light shading). (e) to (h) show mean and variability of stratospheric temperature (averaged between 100 and 10 hPa) from UKMO (solid line and light shading), ECMWF (dash-dotted line and line-shading), and UMCHEM (dashed line and dots) at the same four latitudes. (Where dots are used to show range, each one is an individual monthly mean value.)

Figure 7 shows the correlations of CH_4 versus N_2O and NO_y versus N_2O in January and October after 8 years of UMCHEM simulation. These tracer–tracer plots were generated using one instantaneous sample of the chemical species at a particular time step. Essentially, after 5 years' simulation, the compact correlations are very strong and there is very little variation in the correlation between these species throughout the year (Sankey and Shepherd 2003). The data from the UMCHEM also show little seasonal variation in the CH_4 versus N_2O correlation. However, some seasonal difference can be noted in NO_y versus N_2O correlations. At the SH higher altitudes, the compactness is not very strong and the points in the higher altitudes show some evidence of spreading particularly in October. The similar feature also existed in the corresponding plots from the CCM described by Sankey and Shepherd (2003) and they argued that the conversion

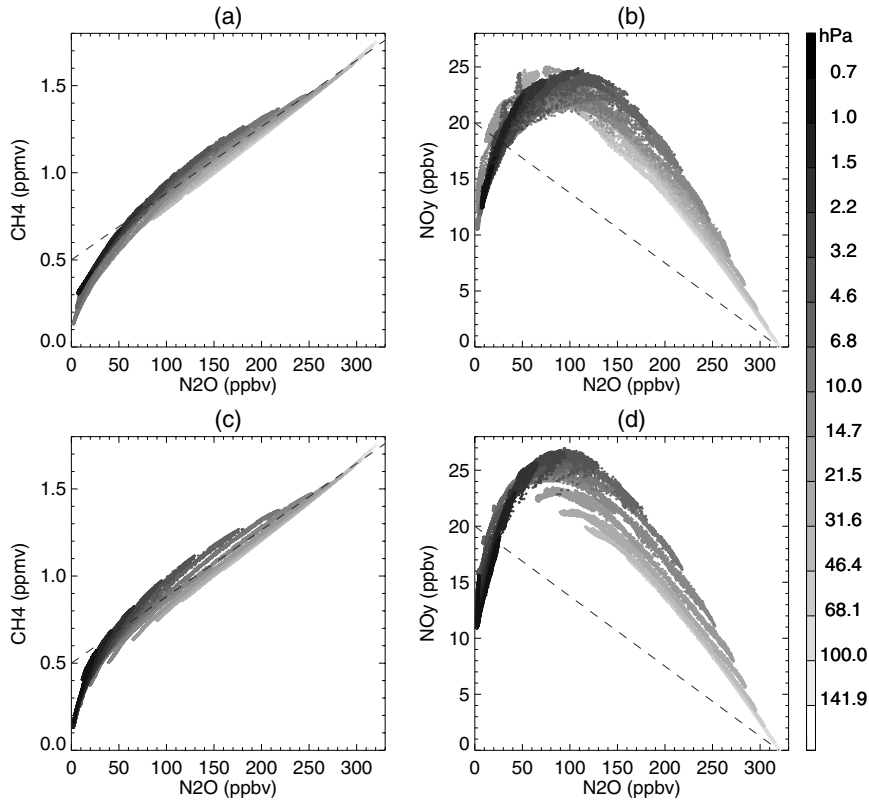

Figure 7. Tracer–tracer correlation plots of (a) N_2O versus CH_4 and (b) N_2O versus NO_y for January northern hemisphere from the UMCHEM run **R0** after 8 years of simulation. (c) and (d) are as (a) and (b), but for October. (e) to (h) are as (a) to (d), but for the southern hemisphere. Different grey shades represent data from different model levels. The dashed lines are fits to ER-2 observations for the lower stratosphere (see Kawa *et al.* 1993).

of N_2O to NO_y is more rapid at higher altitudes and so the conditions for compact correlation are violated.

Not only is a broadly compact correlation achieved by the model, the slope of CH_4 versus N_2O is reasonably consistent with observational fit (Kawa *et al.* 1993). However, the slope of the UMCHEM NO_y versus N_2O correlation is much larger (by a factor of 2) than the observations. For long-lived chemical species the slope of the correlation depends on chemistry (Sankey and Shepherd 2003). We have noted from Figs. 4 and 5 that the model stratospheric chemistry behaves well compared with observations. Here the slope of the UMCHEM CH_4 versus N_2O being in good agreement with observations further indicates that the chemistry in the UMCHEM is reasonable.

For correlations between NO_y versus N_2O, it is thought the slope is mainly determined by the chemistry while compactness of the correlation is related to the mixing process. Figure 7 shows that NO_y mixing ratios are much higher than observations. Rinsland *et al.* (1999) reported that the lack of low NO_y values may be due to denitrification which is not included in the UMCHEM runs. However, it is also believed that low mixing ratios of NO_y are related to the dynamical processes which mix the air brought down from above across the polar vortex barrier (Michelsen *et al.* 1998).

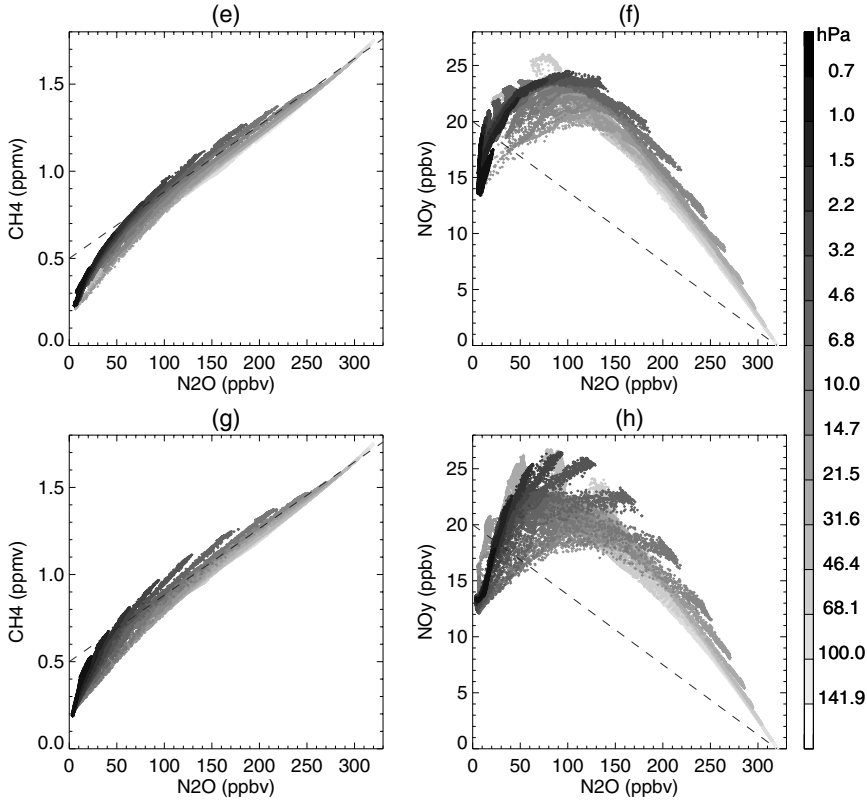

Figure 7. Continued.

The corresponding plots based on the data from the SLIMCAT run are shown in Fig. 8. In contrast to the UMCHEM, a stronger seasonal variation in the correlation between CH_4 and N_2O can be noted, and also between NO_y versus N_2O correlations. The isentropic levels used in the stratosphere in SLIMCAT lead to a separation of correlation curves which is not seen so clearly in the pressure-level UMCHEM. For NO_y versus N_2O, SLIMCAT gets a better representation of the observed correlation slope. SLIMCAT also produces a strong signal of denitrification in the SH in October as this run included the sedimentation of PSCs.

Figures 7 and 8 together suggest that the much higher slope of the UMCHEM NO_y versus N_2O correlation is due largely to too strong vortex confinement (as is implied in Fig. 1) rather than to the denitrification which is not considered in the UMCHEM but is in SLIMCAT.

4. Effect of chemistry coupling

(*a*) *Coupling of O_3, N_2O and CH_4*

As mentioned above, the UM has been used in many studies of the middle atmosphere but the fields used in the radiation calculations, and the coupling between chemistry and radiation, have varied. In the full chemistry runs of Austin and co-workers (e.g. Austin *et al.* 2001), the only species coupled to the radiation scheme was O_3. The other species in the radiation calculation (i.e. minor GHGs such as N_2O, CH_4,

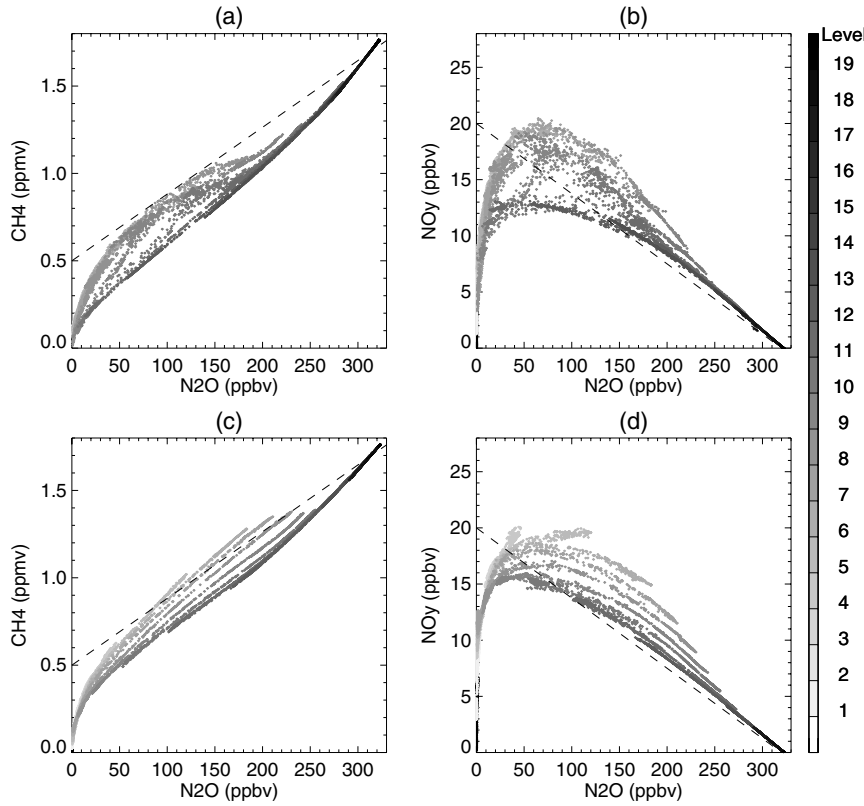

Figure 8. As Fig. 7, but for data from the SLIMCAT CTM run.

CFC11 and CFC12) were specified from observations or predicted future scenarios independent of the chemistry. For water vapour they used the UM's humidity field but with the addition of a contribution from methane oxidation. Again, however, this was different to the H_2O in their chemical scheme.

More recently, Mackenzie and Harwood (2004) coupled O_3, N_2O, CH_4, and H_2O to the UM radiation scheme. However, they did not discuss the effects of this coupling and their chemistry scheme was simplified. As shown below, an accurate prediction of these radiatively active chemical species is crucial to studies of stratospheric chemistry processes.

Braesicke and Pyle (2003) tested the different coupling to the radiation scheme of ozone either from their parametrized chemistry scheme or from a zonal mean climatology derived from their coupled run. They showed that the UM stratosphere was significantly warmer when using its fixed ozone climatology than when using interactive ozone from chemistry scheme. In their study, there was no account of the coupling of water vapour and other chemical species.

Figure 9 shows the differences in zonal mean temperature and zonal wind climatology between the control run **R0** and the basic UM run **UMC**. Note that the temperature from the UMCHEM is about 4 K lower in the Antarctic lower stratosphere than that from the UM; apparently the cold pole problem is also related the chemistry coupling in the model. The maximum ozone mixing ratio of the ozone climatology in the UM run **UMC** is about 4 ppmv larger than the corresponding values calculated in the UMCHEM

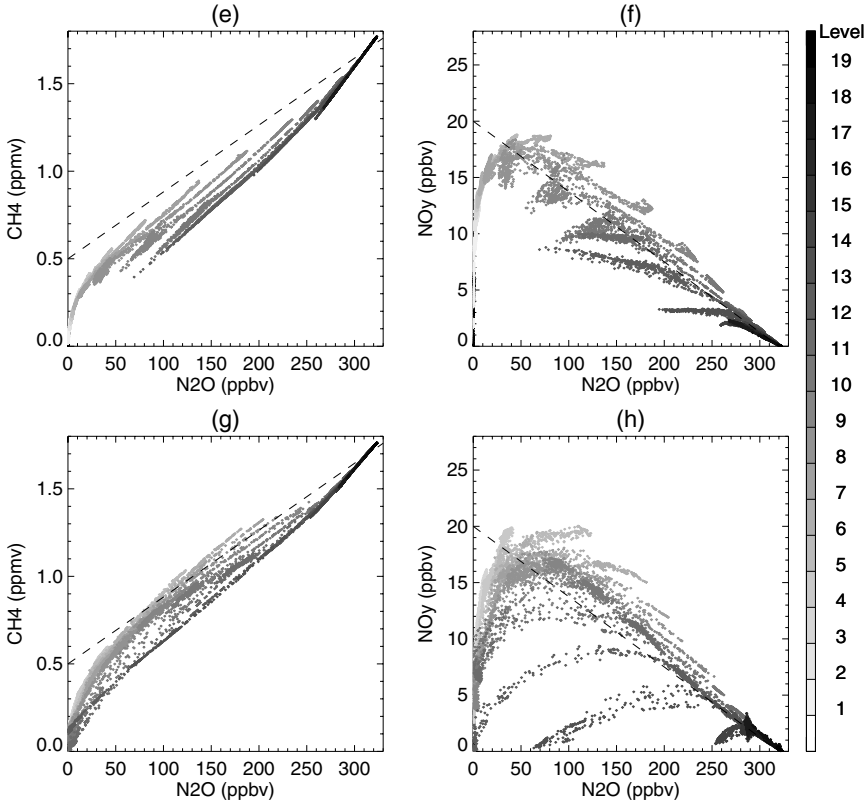

Figure 8. Continued.

control run **R0**. As a result, we get a warmer upper stratosphere and also a warmer (pronounced in the Antarctic), slightly weaker (zonal winds are up to 5 m s^{-1} lower in the southern high latitudes) polar vortex in the basic UM run.

It is evident that the model temperature climatology in the stratosphere is highly sensitive to the ozone field used in the model. An accurate prediction of stratospheric ozone from chemistry schemes is also likely a sensitive factor in resolving the 'cold pole bias' in CCMs and an unreasonable prediction of ozone in polar stratosphere may either intensify or weaken the cold pole bias.

Figure 10 shows the differences in mean age from the UMCHEM run (**R0**) and the basic UM run **UMC**. There are evident differences in the mean ages due to the chemical coupling caused by changes in the strength of the meridional circulation in the two experiments. The air is younger in the UM compared to UMCHEM, particularly in the lower stratosphere where the difference is more than 3 months. The differences in the circulation are mainly due to ozone-induced radiative forcing. Higher ozone concentrations in the stratosphere in the UM run **UMC** give rise to a warmer stratosphere, especially a warmer Antarctic polar vortex in the lower stratosphere. The warmer and weaker polar vortex corresponds to a stronger Brewer–Dobson circulation in the lower stratosphere as the age of air in **UMC** is less than that in UMCHEM. In the upper stratosphere, it appears that the Brewer-Dobson circulation in **UMC** is weaker and the age of air is greater than that of UMCHEM. This could be related to the stronger vertical temperature gradient in the **UMC**.

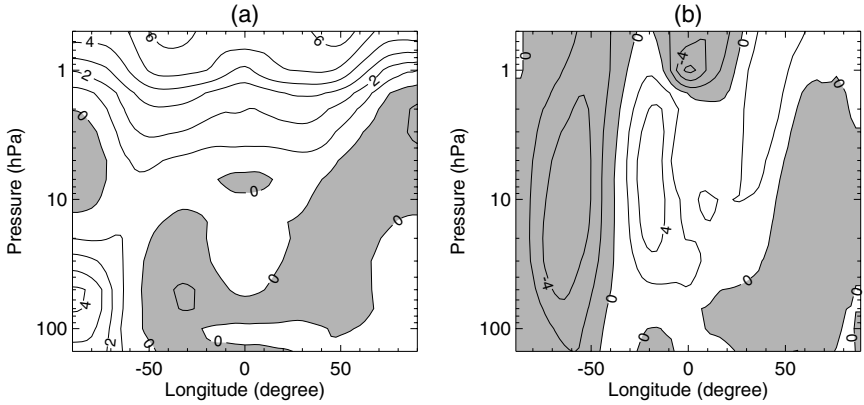

Figure 9. Difference between the basic UM run **UMC** and the UMCHEM control run **R0** for (a) zonal mean temperature (K) and (b) zonal mean wind speed (m s^{-1}) . Negative values are shaded.

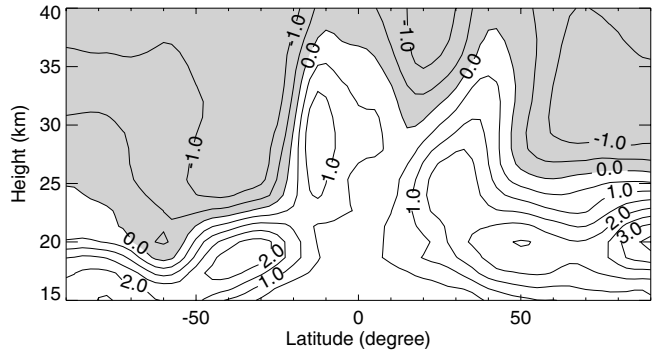

Figure 10. Zonal mean age difference (months) between the UMCHEM (run **R0**) and the basic UM (run **UMC**). Negative values are shaded.

Figure 11 shows the correlation of N_2O mixing ratios from the control run **R0** and the mean ages from run **R0** and **UMC**. Note that both runs have the same tracer advection scheme. It is apparent that there is younger air in both hemispheres in run **R0** when compared to the air without chemistry coupling. In the northern hemisphere, for a given amount of N_2O, air is shifted towards a younger age in **R0**. This is also generally the case in the SH although some of the most aged points in run **R0** have similar age to run **UMC**.

(*b*) *Water vapour coupling*

Our CCM experiments have used different H_2O fields in the radiation scheme, i.e. with and without the coupling of stratospheric H_2O. Here we investigate the differences, especially in the stratospheric ozone field, caused by this coupling of water vapour into the radiation scheme. It is worth noting here that, if the water vapour from chemistry is not coupled in the radiation scheme, then the UM humidity field is used instead. Figure 12 shows the UM specific humidity, q_{um}, and stratospheric chemistry water vapour, q_{chem}, in the control run **R0** and run **R2**. The two water vapour fields are different both in magnitude and in spatial distribution. The q_{chem}values are about twice as large as those of q_{um}, which ignores oxidation of CH_4 as a source of

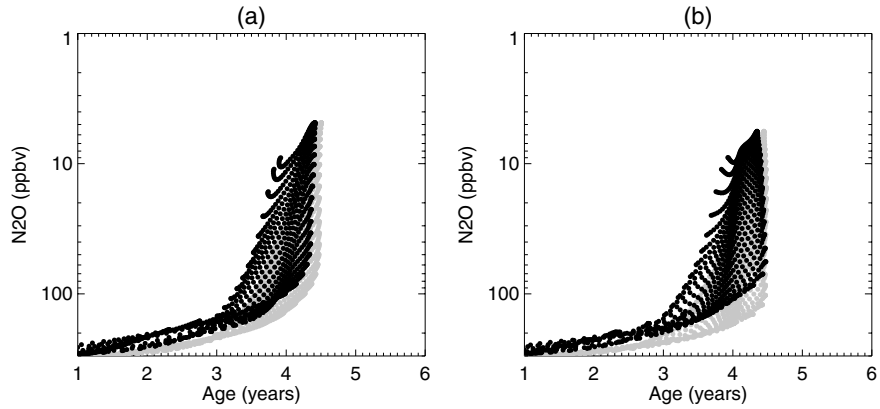

Figure 11. Correlation plots of zonal mean N_2O volume mixing ratio (ppbv) versus mean age (years) for the control run **R0** (black dots) and the basic UM run **UMC** (grey dots) in the (a) northern and (b) southern hemisphere. As N_2O output is only available on the 30 'chemistry' levels in the coupled model (from about 150 to 0.5 hPa), points with low N_2O loading (i.e. the very upper stratosphere) are not shown.

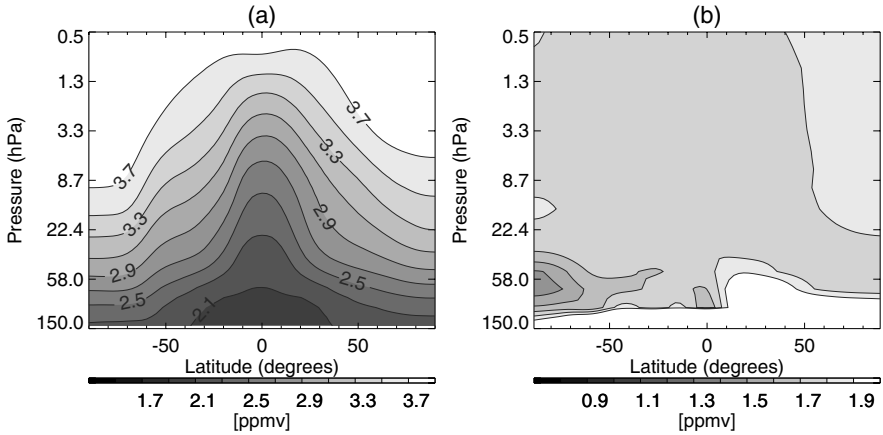

Figure 12. Zonal mean (a) water vapour (q_{chem}, ppmv) from run **R2** and (b) humidity (q_{um}, ppmv) from run **R0**.

stratospheric H_2O. Clearly, the chemistry scheme gives more reasonable water vapour than the UM humidity field in the stratosphere. However, the q_{chem} field does not include large values in the troposphere (to avoid the need to add physical dehydration processes to the chemical tracers) so q_{um} is clearly more realistic here.

The differences in the water vapour fields in Fig. 12 give rise to significant differences in temperature, CH_4 and O_3 between **R0** and **R2** (Figs. 13 and 14). Using the humidity field from UM in the radiation scheme in the stratosphere results in 1–2 K cooling in the stratosphere compared with using the chemistry water vapour field. A maximum difference of around 50 ppbv in CH_4 occurs in the tropical upper stratosphere and the Arctic middle stratosphere, while in the lower stratosphere the differences are only around 1 ppbv. The water vapour coupling also leads to a maximum difference of about 250 ppbv in ozone mixing ratios in the tropical and southern higher latitude upper stratosphere. In the tropical lower stratosphere, a maximum difference of

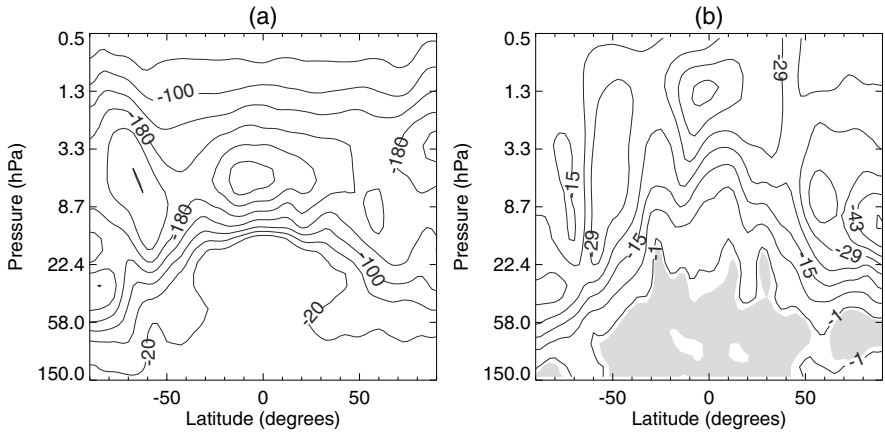

Figure 13. Difference between runs **R0** and **R2** in (a) zonal mean O_3 and (b) zonal mean CH_4 volume mixing ratios (ppbv). Positive values are shaded.

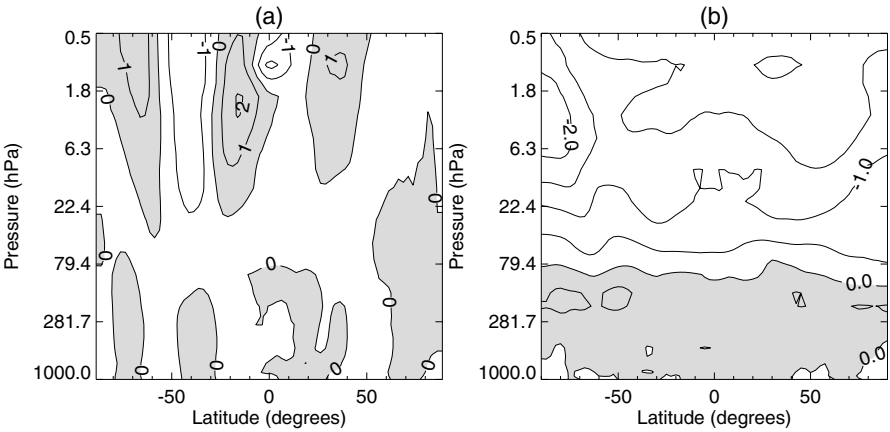

Figure 14. Differences between runs **R2** and **R0** in (a) zonal wind (m s^{-1}) and (b) zonal mean temperature (K). In run **R2** the stratospheric chemistry H_2O (q_{chem}) was coupled to the radiation scheme at altitudes above 80 hPa. Positive values are shaded.

about 30 ppbv occurs in ozone, with the opposite sign to those in the middle and upper stratosphere.

The differences in the zonal circulation between **R0** and **R2** are not very significant; however, we can note that CH_4 concentrations in **R0** are overall smaller than those in **R2** implying that residual circulation in **R0** is weaker than that in **R2**. As a result of this, ozone concentrations are larger in the lower stratosphere in **R0** than in **R2**. In the upper stratosphere the higher temperatures in run **R0** cause less ozone through a direct chemical feedback.

Clearly, coupling of H_2O from the chemistry scheme into the radiation scheme is not only desirable but also important to give a more reasonable prediction of ozone depletion.

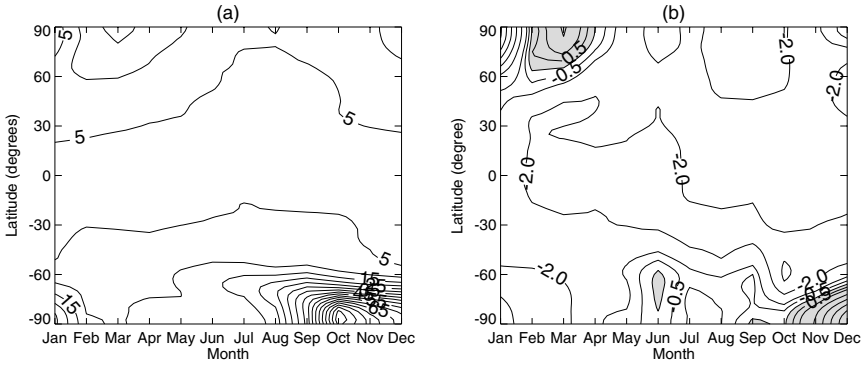

Figure 15. Differences between runs **R4** and **R0** in (a) total-column ozone (%, with contour interval 5%) and (b) zonal mean temperature (K, with contour interval 1 K and +/−0.5 K contours also shown). The temperature has been averaged between 100 and 10 hPa, and positive values are shaded.

5. OZONE RECOVERY

A motivation for creating this coupled radiative–chemical–dynamical model is to use it to predict the future evolution of the stratosphere. The comparisons shown above indicate that the model performs well in simulating present-day conditions. However, accurate predictions of the future depend not only on this but also on a realistic assumption about future trace-gas loadings. Moreover, the relative importance of certain processes, which have not been sufficiently tested under present-day conditions, may increase. For these reasons, future predictions will always need to be updated using the best, most recent model and cover a range of possible assumptions. In this section we discuss a coupled simulation for the year 2050, not as a specific prediction of the future but in order to see whether our model reproduces the expected chemistry–climate coupling.

Figure 15 gives temperature and ozone differences between **R4** and **R0**. In 2050 the model indicates the column O_3 will be increased by around 5% in the tropics and by 15% in the NH high-latitude winter. The largest increase is naturally in the smaller Antarctic ozone hole where the column increase is up to 85% of year 2000 values. Overall the increase in GHGs leads to a cooling of the lower stratosphere of around 2 K, with the exception of two regions which indicate a warming (in high-latitude winter/spring). In the SH, the decreased O_3 loss means a stronger heating in late spring/summer. In the NH the temperature increase does not correlate so clearly with the more modest ozone change—indicating a possible dynamical effect.

The time evolution of vortex-averaged temperature and ozone from UMCHEM control run **R0** for the Arctic and Antarctic are given in Fig. 16, along with their differences from the corresponding fields of run **R4**. Figure 16 shows clearly that temperatures in the Antarctic lower stratosphere are higher due to ozone recovery in the Antarctic summer. In Arctic winter in the mid-stratosphere above 550 K, a significant cooling can be noted, while a slight warming occurs in the lower stratosphere in the Arctic autumn.

An interesting point from Fig. 16 is that the ozone changes between the two experiments are not simply related to the temperature changes in their vertical and time distribution. Compared to that of 2000, the Antarctic maximum ozone increase in 2050 starts in May in the upper stratosphere and moves downward with time and reaches its highest about 1 ppmv in the Antarctic summer. Despite the significant ozone increase

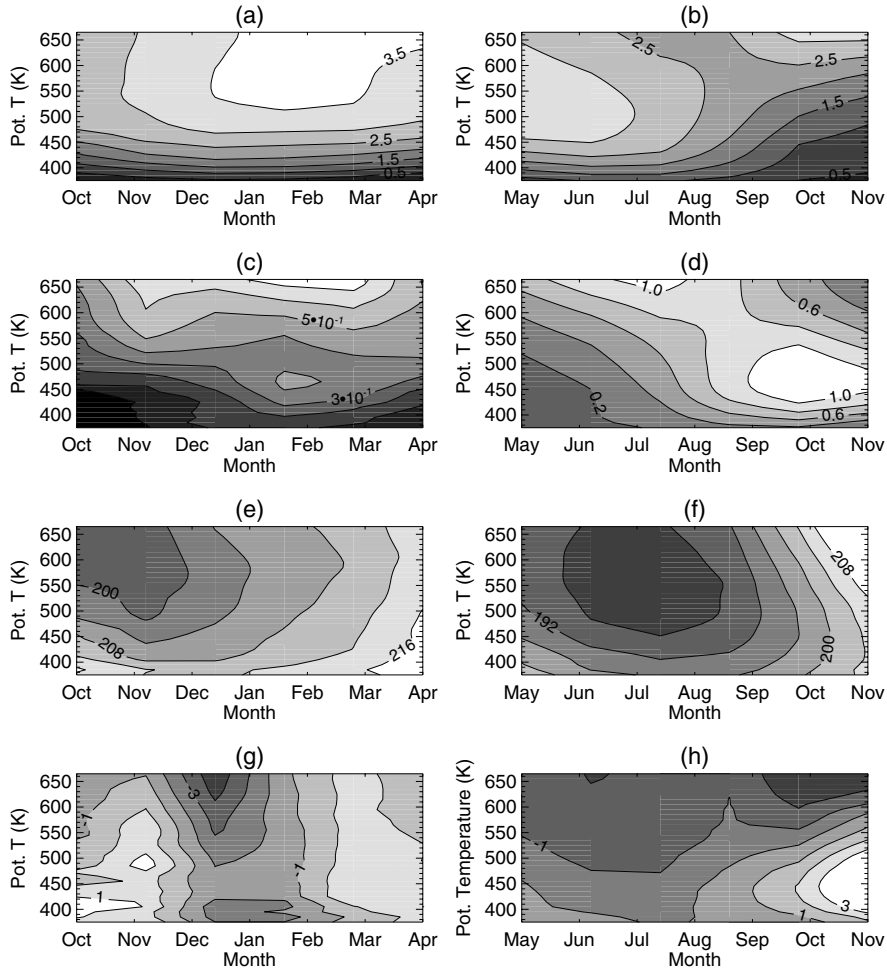

Figure 16. Time–height evolution of vortex-mean ozone from run **R0** for the (a) northern and (b) southern hemisphere (with contour interval 0.5 ppmv), and the differences between runs **R4** and **R0** for the (c) northern and (d) southern hemisphere (with contour interval 0.1 ppmv). (e) to (h) are as (a) to (d), but for temperature, with contour interval 4 K for temperature and 1 K for differences. The vortex boundary was taken as the 65° equivalent potential vorticity latitude contour.

in the upper stratosphere in the Antarctic summer, the Antarctic vortex temperature in **R4** is about 1 K lower than that in **R0** in the upper stratosphere. In 2050 in the Arctic, a significant cooling ranging from 1 to 4 K occurs in the upper stratosphere in winter, while the ozone mixing ratio is increased relative to 2000 by 0.6 ppmv at its maximum. The inference then is that there is not only feedback between future changes in the polar temperature and ozone, but also interaction with other GHGs in a complex chemical, radiative and dynamical interposition.

6. Discussion and conclusions

We have created a new interactive model for coupled chemistry–climate studies of the stratosphere and used it to study the effect of chemical–radiative coupling for trace gases including H_2O under 2000 and 2050 conditions. The model combines the detailed

stratospheric chemistry modules developed and tested in the SLIMCAT/TOMCAT off-line CTMs with a version of the Met Office Unified Model. The resulting UMCHEM chemistry–climate model has a detailed description of stratospheric gas-phase and heterogeneous chemistry.

The UMCHEM model performs well in reproducing basic features of the stratosphere. The distribution of long-lived tracers and age of air compare well with observations. For O_3, the model tends to underestimate the stratospheric column at high latitudes by ~20 DU. This is due to an underestimate of poleward transport in the mid-low stratosphere. The UMCHEM reproduces the seasonal cycle in monthly mean column O_3 well at mid-high latitudes through the variability is slightly smaller than observations and smaller than in the SLIMCAT CTM. Other comparisons with the CTM, which has an identical chemistry scheme, show differences resulting from the models' meteorologies. For example, while the CTM reproduces the observed NO_y versus N_2O correlation, the UMCHEM overestimates the slope by about a factor 2.

Compared to the basic UM, important differences are seen in the UMCHEM climatology. The age of air is less in the basic UM by about 1–3 months in the lower stratosphere but slightly more in the upper stratosphere. A maximum 4 ppmv difference between the prescribed zonal mean ozone climatology in UM and that from the UMCHEM corresponds to a maximum 4 K temperature difference in the Antarctic lower stratosphere. Coupling of the more realistic stratospheric chemistry water vapour warms the model stratosphere by ~1–2 K. Also due to water vapour coupling, the ozone mixing ratios are decreased by a maximum of about 250 ppbv in the tropical and southern higher latitude upper stratosphere, while in tropical lower stratosphere ozone concentrations are increased with a maximum difference of about 30 ppbv. Coupling of H_2O from the chemistry scheme into the radiation scheme allows the model to capture an important feedback and should lead to better predictions of future ozone.

For 2050 conditions, the model produces a column O_3 increase of 5% of its present-day value in the tropics, about 15% in the Arctic winter/spring and up to 90% in the much smaller Antarctic O_3 hole. This large O_3 increase more than offsets the GHG-induced cooling in the Antarctic late spring. In the future the model will be further developed and used to perform time-dependent predictions of the future evolution of the stratosphere.

ACKNOWLEDGEMENTS

This research was supported by the UK Natural Environment Research Council UTLS-O3 programme and the UK Universities' Global Atmospheric Modelling Programme. We thank J. Kettleborough, A. Iwi, P. Braesicke, D. Jackson and J. Cole for help with the UM. We acknowledge use of the TOMS data and SPARC climatologies. We thank the two anonymous referees for their comments.

REFERENCES

Austin, J. 2002 A three-dimensional coupled chemistry-climate model simulation of past stratospheric trends. *J. Atmos. Sci.*, **59,** 218–232

Austin, J., Butchart, N. and Shine, K. P. 1992 Possibility of an Arctic ozone hole in a doubled-CO_2 climate. *Nature*, **360,** 221–225

Austin, J., Butchart, N. and Knight, J. 2001 Three-dimensional chemical model simulations of the ozone layer: 2015–2055. *Q. J. R. Meteorol. Soc.*, **127,** 959–974

Austin, J., Shindell, D., Bruhl, C., Dameris, M., Manzini, E., Nagashima, T., Newman, P., Pawson, S., Pitari, G., Rozanov, E., Schnadt, C. and Shepherd, T. G. 2003 Uncertainties and assessments of chemistry-climate models of the stratosphere. *Atmos. Chem. Phys.*, **3,** 1–27

Ayers, G. P., Gillett, R. W. and Gras, J. L. 1980 On the vapor pressure of sulfuric acid. *Geophys. Res. Lett.*, **7,** 433–436

Braesicke, P. and Pyle, J. A. 2003 Changing ozone and changing circulation in northern mid-latitudes: Possible feedbacks? *Geophys. Res. Lett.*, **30,** 1059, doi:10.1029/2002GL015973

Carslaw, K. S., Luo, B. and Peter, T. 1995a An analytic expression for the composition of aqueous HNO_3–H_2SO_4 stratospheric aerosols including gas phase removal of HNO_3. *Geophys. Res. Lett.*, **22,** 1877–1880

Carslaw, K. S., Clegg, S. L., and Brimblecome, P. 1995b A thermodynamic model of the system HCl–HNO_3–H_2SO_4–H_2O, including solubilities of HBr, from <200 K to 328 K. *J. Phys. Chem.*, **99,** 11557–11574

Chipperfield, M. P. 1999 Multiannual simulation with a three-dimensional chemical transport model. *J. Geophys. Res.*, **104,** 1781–1805

Chipperfield, M. P. and Feng, W. 2003 Comment on: Stratospheric ozone depletion at northern mid-latitudes in the 21st century: The importance of future concentrations of greenhouse gases nitrous oxide and methane. *Geophys. Res. Lett.*, **30,** 1389, doi:10.1029/2002GL016353

Cullen, M. J. P. 1993 The unified forecast/climate model. *Meteorol. Mag.*, **122,** 81–94

Duck, T. J., Whiteway, J. A. and Carswell, A. I. 2001 The gravity wave-Arctic stratospheric vortex interaction. *J. Atmos. Sci.*, **58,** 3581–3596

Edwards, J. M. and Slingo, A. 1996 Studies with a flexible new radiation code. I: Choosing a configuration for a large-scale model. *Q. J. R. Meteorol. Soc.*, **122,** 689–719

Gregory, D. G., Shutts, G. J. and Mitchell, J. R. 1998 A new gravity wave drag scheme incorporating anisotropic orography and low-level wave breaking: impact upon the climate of the UK Meteorological Office unified model. *Q. J. R. Meteorol. Soc.*, **124,** 463–494

Gregory, A. R. and West, V. 2002 The sensitivity of a model's stratospheric tape recorder to the choice of advection scheme. *Q. J. R. Meteorol. Soc.*, **128,** 1827–1846

Hall T. M., Waugh, D. W., Boering, K. A. and Plumb, R. A. 1999 Evaluation of transport in stratospheric models. *J. Geophys. Res.*, **104,** 18815–18839

Hanson, D. and Mauersberger, K. 1988 Laboratory studies of the nitric acid trihydrate: Implications for the south polar stratosphere. *Geophys. Res. Lett.*, **15,** 855–858

Hein, R., Dameris, M., Schnadt, C., Land, C., Grewe, V., Kohler, L., Ponater, M., Sausen, R., Steil, B., Landgraf, L. and Bruhl, C. 2001 Results of an interactively coupled atmospheric chemistry-general circulation model: comparison with observations. *Ann. Geophysicae*, **19,** 435–457

Intergovernmental Panel on Climate Change 2001 *Climate change 2001: the scientific basis.* Eds. J. T. Houghton, Y. Ding, D. J. Griggs, M. Noguer, P. J. van der Linden, X. Dai, K. Maskell and C. A. Johnson, Cambridge University Press, UK

Jackson, D. R., Austin, J. and Butchart, N. 2001 An updated climatology of the troposphere-stratosphere configuration of the Met Office's Unified Model. *J. Atmos. Sci.*, **58,** 2000–2008

Kawa, S. R., Plumb, R. A. and Schmidt, U. 1993 Simultaneous observations of long-lived species. Chapter H: The atmospheric effects of stratospheric aircraft. Report of the 1992 models and measurements workshop. NASA Ref Publ. 1292, Goddard Space Flight Center, Greenbelt, USA

Lary, D. J. and Pyle, J. A. 1991 Diffuse radiation, twilight and photochemistry. *J. Atmos. Chem.*, **13,** 373–392

Logan, J. A. 1999 An analysis of ozone sonde data for the troposphere recommendations for testing 3-D models, and development of a gridded climatology for tropospheric ozone. *J. Geophys. Res.*, **104,** 16115–16149

MacKenzie, I. A. and Harwood, R. S. 2004 Middle-atmospheric response to a future increase in humidity arising from increased methane abundance. *J. Geophys. Res.*, **109,** doi:10.1029/2003JD003590

Manney, G. L., Lahoz, W. A., Sabutis, J. L., O'Neill, A. and Steenman-Clark, L. 2002 Simulations of fall and early winter in the stratosphere. increased methane abundance. *Q. J. R. Meteorol. Soc.*, **128,** 2205–2237

Manzini, E. and McFarlane, N. A. 1998 The effect of varying the source spectrum of a gravity wave parameterization in a middle atmosphere general circulation model. *J. Geophys. Res.*, **103,** 31523–31539

Meier, R. R., Anderson, D. E. and Nicolet, M. 1982 Radiation field in the troposphere and stratosphere from 240-1000 nm. I: General analysis. *Planet. Space Sci.*, **30,** 923–933

Michelsen, H. A., Manney, G. L., Gunson, M. R. and Zander, R. 1998 Correlations of stratospheric abundances of NO_y O_3, N_2O and CH_4 derived from ATMOS measurement. *J. Geophys. Res.*, **103,** 28347–28359

Nagashima, T., Takahashi, M., Takigawa, M. and Akiyoshi, H. 2002 Future development of the ozone layer calculated by a general circulation model with fully interactive chemistry. *Geophys. Res. Lett.*, **29,** doi:10.1029/2001GL014026

Nicolet, M., Meier, R. R. and Anderson, D. E. 1982 Radiation field in the troposphere and stratosphere from 240–1000 nm. II: Numerical analysis. *Planet. Space Sci.*, **30,** 935–983

Plumb, R. A. and Ko, M. K. W. 1992 Interrelationships between mixing ratios of long-lived stratospheric constituents.*J. Geophys. Res.*, **97,** 10145–10156

Ramaroson, R., Pirre, M. and Cariolle, D. 1992 A box model for on-line computations of diurnal variations in a 1D model: Potential for application to multidimensional cases. *Ann. Geophys.*, **10,** 416–428

Randel, W. J. 2003 The SPARC intercomparison of middle atmosphere climatologies. Newsletter No. 20, SPARC, Paris, France

Rinsland, C. P., Salawitch, R. J., Gunson, M. R., Solomon, S., Zander, R., Mahieu, E., Goldman, A., Newchurch, M. J., Irion, F. W. and Chang, A. Y. 1999 Polar stratospheric descent of NO_y and CO and Arctic denitrification during winter 1992–93. *J. Geophys. Res.*, **104,** 1847–1861

Sankey, D. and Shepherd, T. G. 2003 Correlations of long-lived chemical species in a middle atmosphere general circulation model. *J. Geophys. Res.*, **108,** doi:10.1029/2002JD002799

Sander, S. P., Friedl, R. R., DeMore, W. B., Ravishankara, A. R., Golden, D. M., Kolb, C. E., Kurylo, M. J., Hampson, R. F., Huie, R. E., Molina, M. J. and Moortgat, G. K. 2000 Chemical kinetics and photochemical data for use in stratospheric modeling. Evaluation No 13, JPL Publ. 00-3, Pasadena, USA

Steil, B., Bruhl, C., Manzini, E., Crutzen, P. J., Lelieveld, J., Rasch, P. J., Roeckner, E. and Kruger, K. 2003 A new interactive chemistry-climate model: 1. Present-day climatology and interannual variability of the middle atmosphere using the model and 9 years of HALOE/UARS data. *J. Geophys. Res.*, **108,** doi: 10.1029/2002JD002971

Swinbank, R. and O'Neill, A. 1994 A stratosphere–troposphere data assimilation system. *Mon. Weather Rev.*, **122,** 686–702

Swinbank, R., Lahoz, W. A., O'Neill, A., Douglas, A., Heaps, A. and Podd, D. 1998 Middle atmosphere variability in the Meteorological Office Unified Model. *Q. J. R. Meteorol. Soc.*, **124,** 1485–1525

Turco, R. P., Toon, O. B. and Hamill, P. 1989 Heterogeneous physicochemistry of the polar ozone hole. *J. Geophys. Res.*, **94,** 16493–16510

World Meteorological Organization 2003 Scientific assessment of ozone depletion: 2002. Global Ozone Research and Monitoring Project, Report no. 47, WMO, Geneva, Switzerland

Waugh, D. W. and Hall, T. M. 2002 Age of stratospheric air: Theory, observations and models. *Rev. of Geophysics*, **40,** doi:10.1029/2000RG00101

Zhong, W. and Haigh, J. D. 2001 An efficient and accurate correlated-k parameterization of infrared radiative transfer for troposphere-stratosphere-mesosphere GCMs, *Atmos. Sci. Lett.*, **1,** doi:10.1006/asle.2000.0022